

Dielectric-relaxation study of alkylicyanobiphenyl liquid crystals using time-domain spectroscopy

T. K. Bose, B. Campbell, and S. Yagihara*

Groupe de Recherche sur les Diélectriques, Département de Physique, Université du Québec à Trois-Rivières, Trois-Rivières, Québec, Canada G9A 5H7

J. Thoen

Laboratorium voor Akoestiek en Warmtegeleiding, Departement Natuurkunde, Katholieke Universiteit Leuven, Celestijnenlaan 200D, 3030 Leuven, Belgium

(Received 22 April 1987)

Time-domain spectroscopy is used to study the complex permittivity of two types of liquid crystals: heptylcyanobiphenyl (7CB) and octylcyanobiphenyl (8CB). The variation of the dominant relaxation frequency values of both 7CB and 8CB as a function of temperature are very similar, showing no influence of the smectic structure in 8CB. The experimental relaxation measurements in the nematic phase agree qualitatively with the existing theory.

INTRODUCTION

In a recent article¹ we applied for the first time the time-domain spectroscopy (TDS) technique to study the dielectric behavior of a liquid-crystalline material. The advantage of TDS over other steady-state methods resides in the fact that it is fast and can cover a wide frequency range (100 kHz–10 GHz) with a single measurement. With the development in data acquisition and signal analysis,²⁻⁶ the precision of the permittivity values obtained with the TDS technique is certainly comparable to those derived from the more traditional frequency-domain methods.

Dielectric measurements have been used to gain important information on the characteristic properties of liquid crystals.⁷⁻⁹ In most cases, however, experiments were carried out at low frequencies (mainly in the kHz range) and have concentrated on the static permittivity. Information on the dynamical behavior which can be obtained from measurements of the complex permittivity as a function of frequency is rather limited. Many liquid crystals show dielectric relaxation phenomena in the megahertz and the low gigahertz range. This is, of course, exactly the range of frequency which can be covered by a single measurement with the present capabilities of the TDS.^{10,11} Earlier,¹ we demonstrated this possibility with complex permittivity measurements on 8CB (octylcyanobiphenyl), mainly in the isotropic phase. In this article we present the results of a complete set of measurements for 8CB as well as for 7CB (heptylcyanobiphenyl). Results for the complex permittivity (parallel and perpendicular to the director in the mesomorphic phases) are reported for large temperature ranges, covering the isotropic and nematic phases for 7CB as well as isotropic, nematic, and smectic-*A* phases for 8CB.

EXPERIMENTAL SETUP

The measurements were taken using a Hewlett-Packard 181 TDR (time-domain reflectometry) system, which includes a 1105A/1106B tunnel diode pulse generator, a two-channel broadband (dc18 GHz) sampling amplifier type 1430 C, and a display memory oscilloscope type 181 A. A Nuclear Data system 4420 was used for data acquisition and processing.

Although the TDR measurements are carried out in the time domain, the analysis is however, simpler, more precise, and broadband if they are converted to the frequency domain.¹² As discussed in the previous work,¹ the TDR configuration best suited to obtain dielectric spectra over a wide frequency range, is the total reflection from a thin sample with an open termination. The complex permittivity ϵ^* for the above configuration is given by

$$\epsilon^* = \epsilon' - j\epsilon'' = \frac{c}{j\omega d} \frac{V_0 - R}{V_0 + R} x \coth x, \quad (1)$$

where ϵ' and ϵ'' are, respectively, the real and imaginary parts of ϵ^* , and V_0 and R are the Laplace transforms of the incident signal $V_0(t)$ and the reflected signal $r(t)$ in the time domain. $x = j\omega d \epsilon^{*1/2}/c$, with d the length of the sample and ω the angular frequency; $c = 1/(L_c C_c)^{1/2}$ is the speed of light, and C_c, L_c are, respectively, the geometric capacitance and inductance per unit length of the line. Although Eq. (1) has been used with success for moderately to strongly polar liquids,¹¹ it is more appropriate to use a difference equation^{10,13} for liquids with low dielectric constants, as in the present case. One uses the difference between the reflection $r_s(t)$ from a standard dielectric of known ϵ_s^* , and the reflection $r(t)$ from the unknown dielectric of permittivity ϵ^* . The difference is given by

$$\epsilon^* - \epsilon_s^* = \epsilon_s^* \frac{R_s - R}{V_0 - R_s} \frac{[1 + j\omega(d\epsilon_s^*/cf_s) - \frac{1}{3}(\omega d/c)^2\epsilon_s^*]}{1 - [j\omega(d\epsilon_s^*/cf_s) - (\epsilon_s/3)(\omega d/c)^2] \frac{R_s - R}{V_0 - R_s}}, \quad (2)$$

with $f = x \coth x$. An important advantage in this case is essentially that $V_0(t) - r(t)$ reaches equilibrium faster than $V_0(t) + r(t)$, and, as a consequence, experimental truncation (due to the finite time window) of the denominator in Eq. (2) can, to a large extent, be avoided. Using air as standard greatly simplifies Eq. (2) with $\epsilon_s^* = 1$ and $f_s = 1$.

In our previous work on 8CB we did not use a magnetic field for the orientation of the director, and as such, most data were obtained for the isotropic phase and some for the ϵ_{\perp}^* in the nematic phase with surface alignment. For the present work, we used an external magnetic field to orient the sample and were able to obtain detailed information on ϵ_{\perp}^* and ϵ_{\parallel}^* in the mesophases. In our experiments we used two different configurations which are schematically represented in Fig. 1. In the first one given in Fig. 1(a), the radial elec-

tric field in the coaxial cell is always perpendicular to the direction of the magnetic field and thus the N (nematic) or SmA (smectic- A) phase results for ϵ_{\perp}^* are obtained. In the second case the measured permittivity ϵ^* is an average value, given by

$$\epsilon^* = (\epsilon_{\perp}^* + \epsilon_{\parallel}^*)/2. \quad (3)$$

From a combination of the results for both configurations, values for ϵ_{\perp}^* and ϵ_{\parallel}^* can thus be obtained separately. Magnetic fields as large as 0.4 T were used in order to arrive at uniformly oriented samples. For the measurements in the SmA phase, the samples were cooled from the nematic phase in the presence of the magnetic field.

The sample cell is a short section of a standard 3.5-mm precision 50- Ω coaxial air line. The length of the sample is determined by the electrical length of the inner conductor of the cell. Its calibration by using known alcohols (ethanol and butanol) gives a length of 7.80 mm. The discussion on the choice of the sample length is given in the previous paper.¹ The dielectric sample is placed between the two conductors of the coaxial air line with the inner radius of 1.5 mm and the outer radius of 3.5 mm.

The temperature of the sample was regulated by means of a flow of water at constant temperature through a jacket around the outer wall of the sample cell (Fig. 1). The temperature of the water was controlled with a Lauda type RC-20 temperature regulator. The sample temperature was measured with a calibrated thermistor. The temperature stability of the sample over the measuring time was $\pm 0.02^\circ\text{C}$. The 7CB and 8CB liquid-crystalline compounds were obtained from BDH Chemicals Ltd. (Poole, Dorset, United Kingdom) and used without further purification.

RESULTS AND DISCUSSION

We have measured the dielectric properties of 8CB and 7CB over the temperature range between 25 and 60°C . The nematic-to-isotropic transition temperature for both compounds is around 42°C and thus in the middle of the measured temperature range. Figure 2 gives typical $\epsilon'(\omega)$ and $\epsilon''(\omega)$ results as a function of the frequency $f = \omega/2\pi$ for 7CB. The results for 8CB are quite similar to the ones given in Fig. 2 for 7CB. It can be seen from Fig. 2 that a large dielectric relaxation occurs in the low MHz range. From Eq. (1) it is possible to calculate the static dielectric constant ϵ_0 by taking the limit $\omega \rightarrow 0$.

In Fig. 3 we have compared our ϵ_0 data for 7CB with values from the literature. There is very good agreement for the whole temperature range with the data by Davies

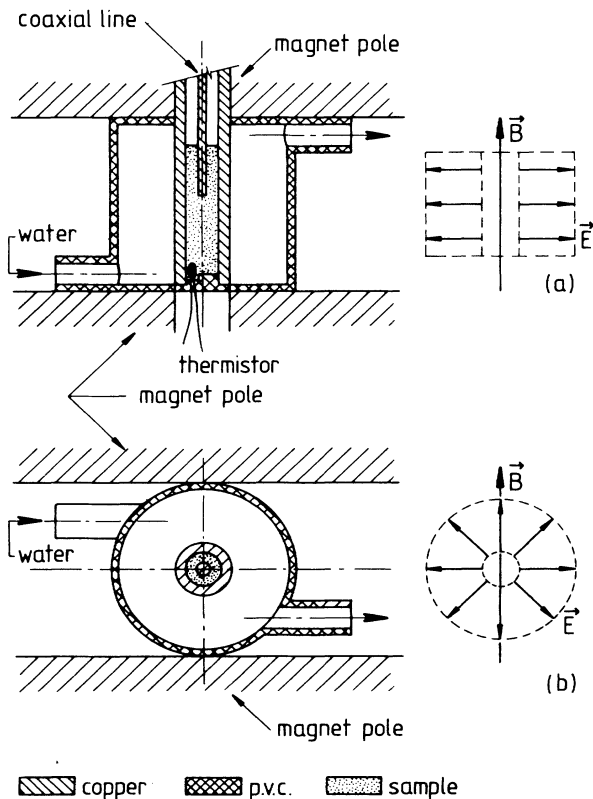


FIG. 1. Schematic diagram of the setup for measuring the orientation dependence of the complex permittivity ϵ^* in the mesophases. (a) Configuration for the perpendicular component of ϵ^* . (b) Configuration giving results for ϵ^* equal to the sum of half the perpendicular and half the parallel component.

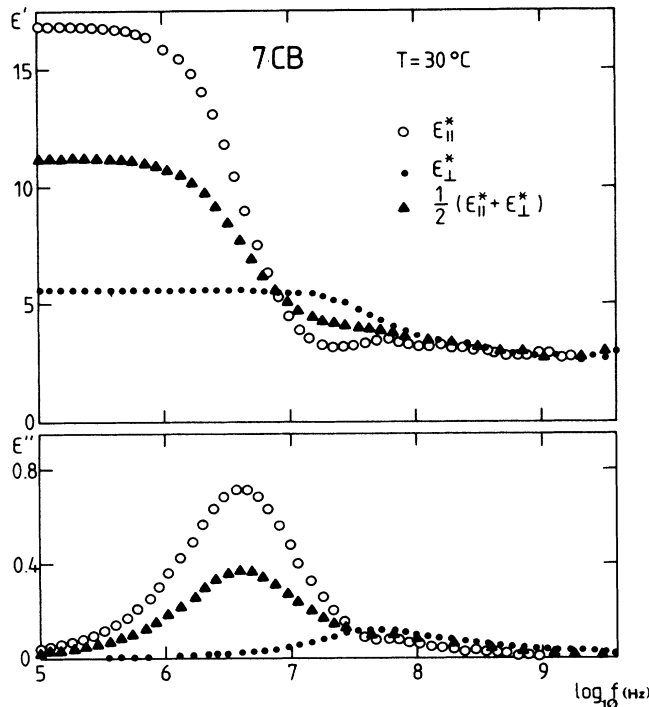


FIG. 2. Frequency dependence of the real and the imaginary parts of the complex permittivity for three different conditions of 7CB.

*et al.*¹⁴ (the pluses) and also with the data by Lippens *et al.*¹⁵ (the open triangles) for $T > 35^\circ\text{C}$. Two data points below 35°C for $\epsilon_{||}$ and ϵ_{\perp} by these authors deviate systematically. A similar comparison for our ϵ_0 data of 8 CB is made in Fig. 4. With the exception of the derived $\epsilon_{||}$ data, our new results are systematically about 2 or 3% lower than the data by Thoen and Menu¹⁶ (the solid curves) and also our earlier results¹ (the pluses). This discrepancy is of the order of the accuracy of the TDS method and can be caused, e.g., by some systematic calibration differences. Sample purity may also play a role. Data by Druon and Wacrenier¹⁷ agree for ϵ_{is} and for ϵ_{\perp} , but are systematically too low for $\epsilon_{||}$. Recently, dielectric results for 8CB have also been published by Buka and Price.¹⁸ A comparison with their ϵ_0 values is very difficult because their results suffer from an unexplained downward shift of 4°C for the transition temperatures in comparison with the rather well-established literature¹⁹ values ($T_{NI} \approx 40.5^\circ\text{C}$ and $T_{NA} \approx 33.5^\circ\text{C}$). Their reference to supercooling in this respect is unjustified for the nematic-smectic-A transition because this transition was shown to be second order.²⁰ If we arbitrarily shift the Buka-Price data up by 4°C , reasonable agreement with the data in Fig. 4 is obtained for ϵ_0 in the isotropic phase as well as for ϵ_{\perp} , but the results for $\epsilon_{||}$ are close to 10% too low.

In Fig. 2 it can be observed that a dominant relaxation mechanism is present in the low MHz region. It can be shown²¹ that successively better approximations for the logarithmic distribution function of relaxation

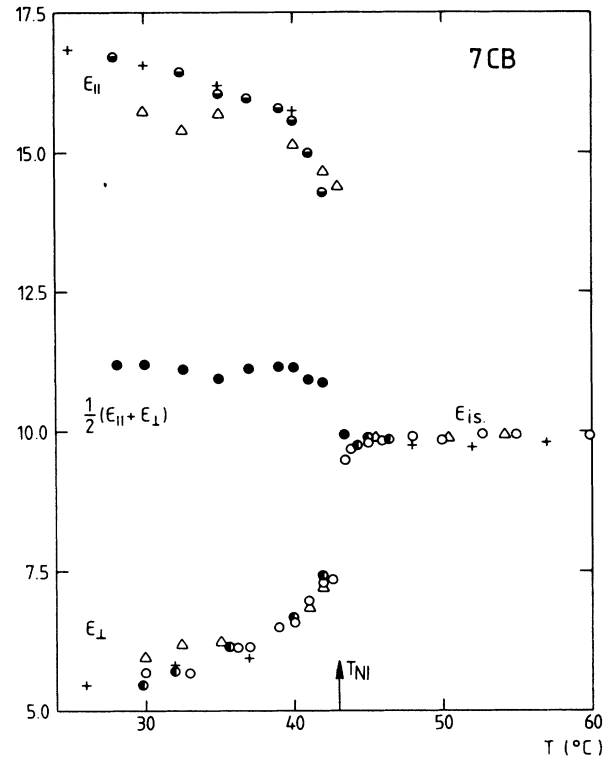


FIG. 3. Temperature dependence of the static dielectric constant (ϵ_{is}) of 7CB in the isotropic phase and in the nematic phase. Open circles are results obtained without a magnetic field, and data with magnetic field always perpendicular to the electric field [see Fig. 1(a)] are indicated with vertically half-filled circles. Solid dots are data with magnetic field in the plane of the electric field [see Fig. 1(b)]. The derived results for $\epsilon_{||}$ are given with horizontally half-filled circles. The open triangles are data by Lippens *et al.* (Ref. 15). The pluses are results by Davies *et al.* (Ref. 14). T_{NI} is the nematic-isotropic transition temperature.

times G ($\ln\tau$) can be obtained from $\epsilon''(\omega)$, $\epsilon'(\omega)$, and their derivatives with respect to $\ln\omega$. The following expressions²¹ are of interest to us here:

$$G_0 = \frac{2\epsilon''(\omega)}{\pi(\epsilon_0 - \epsilon_\infty)}, \quad (4)$$

$$G_1 = -\frac{1}{\epsilon_0 - \epsilon_\infty} \frac{d\epsilon'(\omega)}{d \ln \omega}, \quad (5)$$

$$G_2 = \frac{2}{\pi(\epsilon_0 - \epsilon_\infty)} \left[\epsilon''(\omega) - \frac{d^2\epsilon''(\omega)}{d(\ln\omega)^2} \right]. \quad (6)$$

G_0 is usually called the normalized loss function. If sufficiently detailed and accurate $\epsilon'(\omega)$ and $\epsilon''(\omega)$ results over a large frequency range are available, the above expressions should be very useful in determining different relaxation regimes. We have applied this method to our TDS results for 7CB and 8CB. In Fig. 5 the quantities G_0 , G_1 , and G_2 [defined in Eqs. (4)–(6)] are plotted as a function of frequency for one temperature in the isotropic phase and one in the nematic phase (ϵ_{\perp}^*) for the case

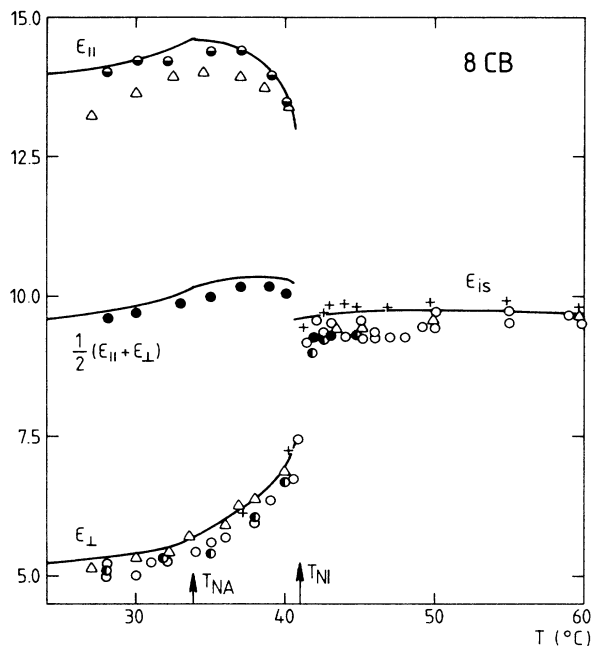


FIG. 4. Temperature dependence of the static dielectric constant (ϵ_{is}) of 8CB in the isotropic, the nematic, and the smectic-*A* phases. Open circles are results obtained without a magnetic field, and data with the magnetic field always perpendicular to the electric field [see Fig. 1(a)] are indicated with vertically half-filled circles. Solid dots are data with the magnetic field in the plane of the electric field [see Fig. 1(b)]. The derived results for ϵ_{\parallel} are given with horizontally half-filled circles. The solid curves represent data by Thoen and Menu (Ref. 16). The pluses are data by Bose *et al.* (Ref. 1). The open triangles are data by Druon and Wacrenier (Ref. 17). T_{NI} is the nematic-isotropic transition temperature and T_{NA} is the nematic-smectic-*A* transition temperature.

of 7CB. In this figure it can be seen that for higher frequencies peaks appear for the higher derivatives, indicating weak relaxation mechanisms in that frequency range. From Fig. 5 it is also clear that the relaxation frequency of the dominant mechanism can be very well localized in this way. A full analysis of all the data has been carried out in this manner. In Fig. 6 (for 7CB) and Fig. 7 (for 8CB) we have plotted the relaxation frequency f_R for the dominant relaxation as a function of $1/T$. A comparison is also made with the limited results from other sources. In general, there is satisfactory agreement, with the exception of the results by Davies *et al.*,¹⁴ for the perpendicular component of 7CB, which are substantially larger. The results by Ratna and Shashidhar²² for the parallel component of 8CB are also on the high side.

In Fig. 8 a comparison has been made between our 7CB and 8CB data for the relaxation frequencies. The data are plotted with the same scale factors for $1/T$, but in such a way that the $1/T$ values for the *NI* transitions of both compounds coincide. Since their T_{NI} values differ by about 1°C, this represents a small shift. Some striking observations can be made from this comparison. First of all, one sees, apart from a very small difference

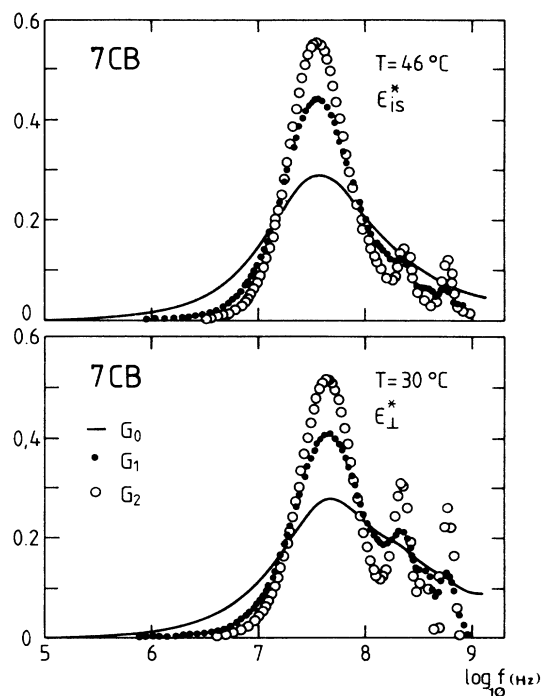


FIG. 5. Frequency dependence of the quantities G_0 , G_1 , and G_2 , defined in Eqs. (4)–(6), for 7CB at one temperature in the isotropic phase ($T=46^\circ\text{C}$) and at one temperature ($T=30^\circ\text{C}$) in the nematic phase for the case of the perpendicular component of the complex permittivity.

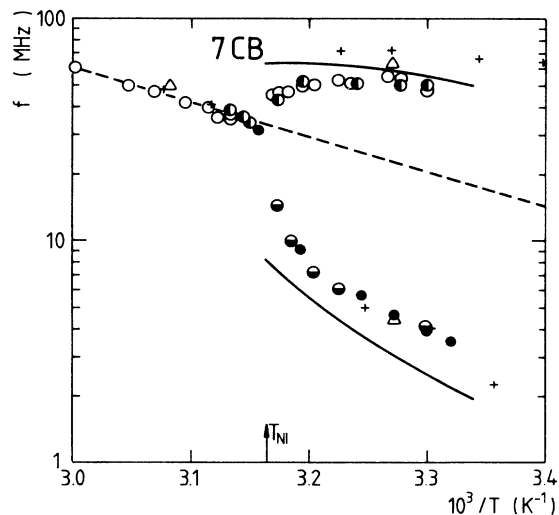


FIG. 6. Temperature dependence of the dominant relaxation frequency for 7CB. The meaning of the circular symbols, representing our data, is the same as for Fig. 3. The pluses are results by Davies *et al.* (Ref. 14), and the open triangles are by Lippens *et al.* (Ref. 15).

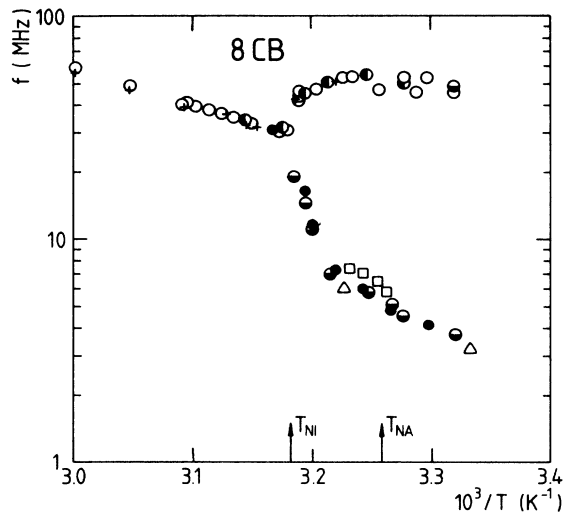


FIG. 7. Temperature dependence of the dominant relaxation frequency for 8CB. The meaning of the circular symbols, representing our data, is the same as for Fig. 5. The pluses are results by Bose *et al.* (Ref. 1), the open triangles are by Druon and Wacrenier (Ref. 17), and the squares by Ratna and Shashidhar (Ref. 22).

in the isotropic phase, almost identical results in the liquid-crystalline phases. The presence of the smectic-*A* phase in 8CB does not make any difference with the results for 7CB which has only a nematic phase. Apparently, the occurrence of the Sm-*A* layering does have little influence on the dynamical behavior of the dipoles. Another observation is the continuous slope change below T_{NI} . It therefore does not make much sense to

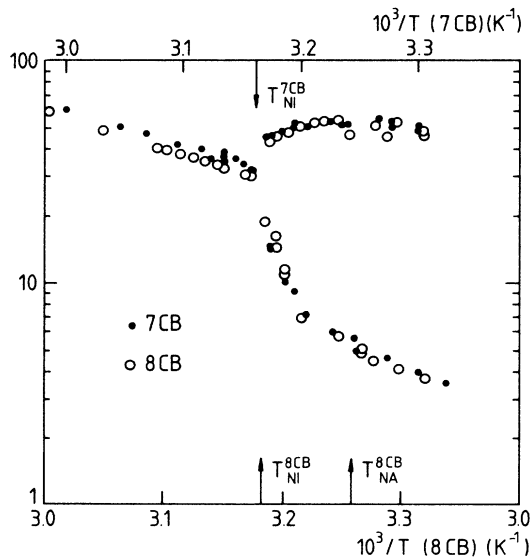


FIG. 8. Comparison between the relaxation frequencies of 7CB and 8CB. A small shift in the temperature scales has been imposed in order to make the isotropic to nematic transition temperatures coincides.

define distinct activation energies for the nematic and the smectic-*A* phases because f_R is not linear in $1/T$. That is, however, what Druon and Wacrenier and also Buka and Price tried to do on the basis of a few data points in each phase. As will be pointed out further, the dominant factor behind this continuous slope change below T_{NI} is related to the presence of the nematic potential, and the temperature dependence of the nematic order parameter.

The analysis of the high-frequency relaxation mechanism on the basis of Eqs. (4)–(6) clearly shows the presence of several peaks both in the isotropic as well as mesomorphic phases (see Fig. 5). In the case of the isotropic phase in 7CB we find three relaxation frequencies: 39, 225, and 550 MHz at 46°C. The higher relaxation frequencies, i.e., 225 and 550 MHz are carried over into the perpendicular component of the nematic phase (Fig. 5). We also observed that within the measured range of temperature these high relaxation frequencies are independent of the temperature in the isotropic phase as well as the nematic phase of 7CB.

The analysis of the high-frequency relaxation mechanism in 8CB reveals a similar situation. We again find three relaxation frequencies in the isotropic phase of 8CB, i.e., 34.3, 225, and 600 MHz at 44.7°C. The three relaxation frequencies are similar to the frequencies of 7CB at 46°C. We notice again that the higher relaxation frequencies of 225 and 600 MHz go over to the perpendicular component of 8CB in the nematic phase and are independent of temperature within the measured temperature range.

Since the secondary relaxation peaks are obtained by using Fourier transform of the time-domain records, there certainly exists the possibility that they could be artifacts resulting from the transformation time frequency. The two possible sources of error are truncation error in the numerical transform or spurious reflections from a mismatch in the coaxial line system. We did not observe any reflection peak arising from the impedance mismatch in the time-domain record. In order to cover the whole frequency range of interest for 7CB or 8CB with a single experiment, we had to compromise on an optimum length (7.8 mm). Under these conditions we could get a maximum time window τ of about 7 ns free of spurious reflections. We were thus able to cover a difference curve $r_s(t) - r(t)$ down to 5–6% of its original value. To approximate the contribution of the remaining area for $t > \gamma$ we added an exponential tail to the difference curve, which at long times varies as $\exp(-t/\tau_c)$, where τ_c is the time constant for charging the sample with static permittivity ϵ_0 and length d through the resistance of the tunnel diode pulse generator. We have tested the extrapolation procedure by starting at different points between 6 and 7 ns and found in all cases very good internal consistency.

The parallel components of both 7CB and 8CB possess only one relaxation frequency. The Cole-Cole plot for $\epsilon_{||}^*(\omega)$ in 7CB (Fig. 9) clearly shows a Debye semicircle.

The theory proposed by Martin, Meier, and Saupe²³ for the dielectric relaxation in the nematic phase gives good qualitative agreement with the experimental values

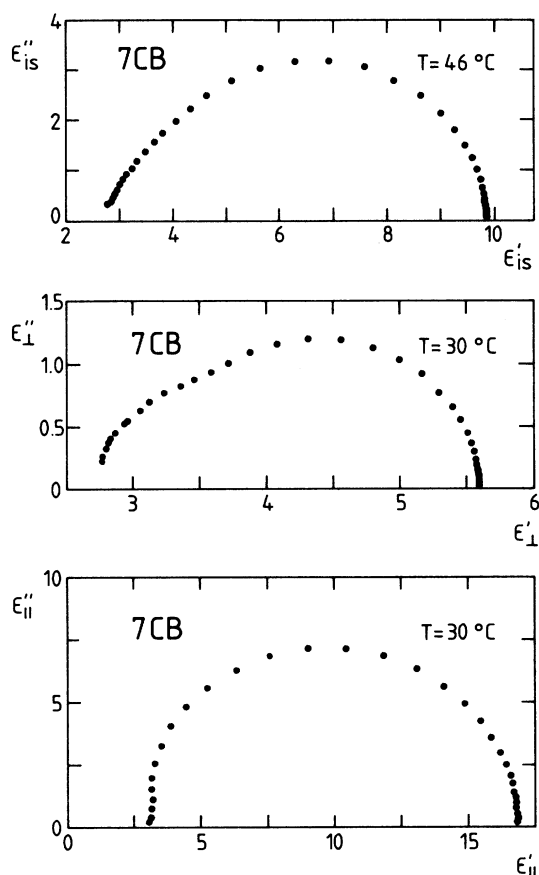


FIG. 9. Cole-Cole plots for 7CB in isotropic, nematic parallel, and nematic perpendicular phases. ϵ'_{is} , ϵ'_{\perp} , ϵ'_{\parallel} , ϵ''_{is} , ϵ''_{\perp} , and ϵ''_{\parallel} are, respectively, the real and imaginary parts of the dielectric constant for the isotropic, nematic perpendicular, and nematic parallel.

(Fig. 6). The relaxation times (τ_{\parallel} and τ_{\perp}) in the nematic phase are given in terms of retardation factors g_{\parallel} and g_{\perp} as $\tau_{\parallel} = g_{\parallel}\tau_0$ and $\tau_{\perp} = g_{\perp}\tau_0$, where τ_0 is the molecular relaxation time in the isotropic phase, extrapolated to the temperature of interest. The retardation factors depend on q/kT , the strength of the nematic potential, where q is the potential barrier height, k is the Boltzmann's constant, and T is the absolute temperature. The retardation factors can be calculated for various values of q/kT or S , the order parameter, as a function of the reduced temperature $TV^2/T_{NI}V_{NI}^2$ where T_{NI} is the nematic-isotropic transition temperature and V is the molar volume.²⁴ The calculated values of the principal relaxation frequency both for the parallel as well as perpendicular components in 7CB are plotted as a function of $1/T$ and compared with the experimental values in Fig. 6. The theoretical curve calculated on the basis of the theory of Martin *et al.*²³ lies somewhat lower than the experimental points for the parallel component, but gives nearly the same temperature variation. The calculated curve of f_R for the perpendicular component of 7CB agrees quantitatively better with the experimental values for the low-temperature range. Also, the theory

does not account properly for the increased curvature of the experimental points close to the nematic-isotropic transition temperature. This is probably due to the fact that the theory overestimates the value of the nematic order parameter near the nematic-isotropic transition.^{16,25} Martin *et al.*²³ also predict for the nematic phase two subsidiary relaxations at higher frequencies. The strength of the subsidiary relaxations for the parallel component is so small that it is not expected to be observable experimentally. Indeed, we find a single relaxation frequency for the parallel component in both 7CB and 8CB. Figure 9 shows that a Cole-Cole plot for $\epsilon'_{\parallel}(\omega)$ in 7CB is a Debye semicircle, in conformity with the theory.

For the perpendicular component in 7CB, the theory of Martin *et al.*²³ predicts two subsidiary relaxation frequencies at around 100 and 250 MHz close to the nematic-isotropic transition temperature. The strength of these secondary relaxations is calculated to be about 10% and 1% of the principal relaxation frequency. These high-frequency relaxations are very weakly temperature dependent. The experimentally observed subsidiary relaxations in the perpendicular component of the nematic phase in 7CB are temperature independent within the measured temperature range and are situated at around 225 and 600 MHz, respectively (Fig. 5), somewhat higher than the predicted values of Martin *et al.*²³ Of the three different relaxation mechanisms in the perpendicular component of $\epsilon^*(\omega)$ below T_{NI} , the dominant low-frequency relaxation can be related quite well with the principal relaxation mechanism predicted by the theory of Martin *et al.*²³ Although the relaxation frequencies of two secondary relaxations are somewhat higher than the ones predicted by Martin *et al.*²³ their temperature dependence is very similar to the theoretical calculation. The existence of the higher-frequency relaxations in the isotropic phase, not predicted by Martin *et al.*,²³ may result from the persistence on a short-range level of sufficient nematic order. As can be seen from Fig. 5, the secondary peaks in the isotropic phase are much lower than those in the nematic phase. It could also be that the secondary relaxations observed in the nematic as well as isotropic phases are associated with intramolecular motions of the molecules.

Finally, Wacrenier *et al.*²⁶ observed a low-frequency relaxation in the perpendicular component of 7CB, comparable to the relaxation frequency of the parallel component of 7CB. This relaxation frequency is not predicted by the theory of Martin *et al.*²³ We do not observe such low-frequency relaxation mechanisms in our experimental results. We believe that the ϵ'_{\perp} results of Wacrenier *et al.*²⁶ were probably caused by an incomplete orientation of the sample, as suggested by Kresse.²⁷

SUMMARY AND CONCLUSIONS

We have carried out dielectric measurements on 8CB and 7CB over a large frequency range in isotropic as well as mesomorphic phases. The experimental data relating to ϵ_{\parallel} give a single relaxation time, in conformity with the theory and other experimental measurements.

Of the three different relaxation mechanisms in the perpendicular component of $\epsilon^*(\omega)$ below T_{NI} , the dominant low-frequency relaxation can be related quite well to the principal relaxation mechanism predicted by the theory of Martin *et al.*²³ The two high-frequency relaxations are temperature independent within the measured range of temperature and appear at frequencies different from the frequencies predicted by the theory of Martin *et al.*²³ From a comparison of the dominant relaxation frequency values for 7CB and 8CB in Fig. 8, we can observe that the occurrence of a smectic phase in 8CB has no noticeable influence on the temperature dependence of its relaxation mechanism. In the case of ϵ_{\perp} we also do not find the low-frequency relaxation observed by

Wacrenier *et al.*²⁶ Since TDS enables one to obtain information over a large frequency range rapidly and at intervals as small as one desires it is ideally suited for the decomposition of the relaxation frequencies.

ACKNOWLEDGMENTS

This work was supported by the government of Quebec through its FCAR funds (Fonds pour l'Aide et le Soutien à la Recherche) and Natural Sciences and Engineering Council of Canada. We would also like to thank the governments of Quebec and Flanders for the grant of an exchange program between our two laboratories.

*Present address: Tokai University Junior College, Tokyo Campus, 2-3-23 Takanawa, Minato-Ku, Tokyo 108, Japan.

¹T. K. Bose, R. Chahine, M. Merabet, and J. Thoen, *J. Phys. (Paris)* **45**, 1329 (1984).

²W. L. Gans and J. R. Andrews, *Nat. Bur. Stand. (U.S.) Tech. Note* **672**, 176 (1975).

³B. J. Elliott, *IEEE Trans. Instrum. Meas.* **25**, 376 (1976).

⁴S. M. Riad and N. S. Nahman, *IEEE Trans. Instrum. Meas.* **25**, 388 (1976).

⁵R. H. Cole, *Ann. Rev. Phys. Chem.* **28**, 283 (1977).

⁶R. Chahine and T. K. Bose, *Rev. Sci. Instrum.* **54**, 1243 (1983).

⁷J. P. Parniex, Ph.D. thesis, Université de Lille, France, 1982.

⁸P. G. de Gennes, *The Physics of Liquid Crystals* (Clarendon, Oxford, 1974).

⁹W. H. de Jeu, in *Liquid Crystals*, edited by L. Liebert (Academic, New York, 1978), Suppl. 14, p. 109.

¹⁰R. Chahine and T. K. Bose, *IEEE Trans. Instrum. Meas.* **32**, 360 (1983).

¹¹R. Chahine and T. K. Bose, *J. Chem. Phys.* **72**, 808 (1980).

¹²R. H. Cole, *J. Phys. Chem.* **79**, 1459 (1975).

¹³R. H. Cole, S. Mashimo, and P. Winsor IV, *J. Phys. Chem.* **84**, 786 (1980).

¹⁴M. Davies, R. Moutron, A. H. Price, M. S. Beevers, and J. Williams, *J. Chem. Soc. Faraday, Trans. 2* **72**, 1447 (1976).

¹⁵D. Lippens, J. P. Parneix, and A. Chapoton, *J. Phys. (Paris)* **38**, 1465 (1977).

¹⁶J. Thoen and G. Menu, *Mol. Cryst. Liq. Cryst.* **97**, 163 (1983).

¹⁷G. Druon and J. M. Wacrenier, *J. Phys. (Paris)* **38**, 47 (1977).

¹⁸A. Buka and A. H. Price, *Mol. Cryst. Liq. Cryst.* **116**, 187 (1985).

¹⁹BDH Chemicals Ltd. Catalogue (Poole, Dorset, U.K., 1979).

²⁰J. Thoen, H. Marynissen, and W. Van Dael, *Phys. Rev. A* **26**, 2886 (1982).

²¹C. J. F. Böttcher and P. Bordewijk, *Theory of Electric Polarisation* (Elsevier, Amsterdam, 1978), Vol. II.

²²B. R. Ratna and R. Shashidhar, *Mol. Cryst. Liq. Cryst.* **42**, 185 (1977).

²³A. J. Martin, G. Meier, and A. Saupe, *Symp. Faraday Soc.* **5**, 119 (1971).

²⁴W. H. de Jeu, *Physical Properties of Liquid Crystalline Materials* (Gordon and Breach, New York, 1980).

²⁵E. F. Gramsbergen, L. Longa, and W. H. de Jeu, *Phys. Rep.* **135**, 197 (1986), and references therein.

²⁶J. M. Wacrenier, C. Druon, and D. Lippens, *Mol. Phys.* **43**, 97 (1981).

²⁷H. Kresse, in *Advances in Liquid Crystals*, edited by G. H. Brown (Academic, New York, 1983), Vol. VI.